J Genet Resour2025; 11(2): 268-276 *Homepage: http://sc.journals.umz.ac.ir/*

RESEARCH ARTICLE *DOI: 10.22080/jgr.2026.31027.1456*

J|G|R

Differential Modulation of Biofilm-associated Gene Expression by Ag and ZnO Quantum Dots in Gram-positive and Gram-negative Bacteria: Implications for Cutaneous Wound Healing

Yasman Sadat Nabipour[1], Ardeshir Hesampour[*1], Salman Ahmady Asbchin[*2], Maryam Tajabadi[1] and Arman Rostamzad[3]

[1] Department of Biology, Faculty of Basic Sciences, Islamic Azad University, Tehran, Iran
[2] Department of Microbiology, Faculty of Science, University of Mazandaran, Babolsar, Iran
[3] Department of Biology, Faculty of Basic Sciences, Ilam University, Ilam, Iran

ARTICLE INFO

Article history:
Received 08 Jun 2025
Accepted 14 Aug 2025
Available 28 Aug 2025

Keywords:
Biofilm
Gene expression
Quantum dots
Wound healing

***Co-corresponding authors:**
✉ A. Hesampour
a.hesampour@gmail.com
✉ S. Ahmady Asbchin
sahmadyas@yahoo.fr

p-ISSN 2423-4257
e-ISSN 2588-2589

ABSTRACT

The rise of multidrug-resistant (MDR) pathogens, particularly biofilm-forming bacteria such as *Acinetobacter baumannii* and *Staphylococcus aureus*, poses a severe threat to global health. Biofilms significantly increase antibiotic resistance and complicate wound infections. This study aimed to synthesize silver quantum dots (Ag-QDs) and zinc oxide quantum dots (ZnO-QDs) using a green hydrothermal method and evaluate their comparative antibacterial, anti-biofilm, and wound-healing efficacy. QDs were synthesized via a hydrothermal method using oak fruit extract as a reducing and stabilizing agent. The nanoparticles were characterized using UV/vis spectroscopy and transmission electron microscopy. The minimum inhibitory concentration (MIC) against clinical and standard strains of *A. baumannii* and *S. aureus* was determined. Anti-biofilm activity was assessed using the microtiter plate assay. The effect of sub-MIC concentrations on the expression of key biofilm-related genes (*bap* and *ompA* in *A. baumannii*; *icaA* and *icaD* in *S. aureus*) was evaluated using Real-time PCR. An in vivo study was conducted on Balb/c mice with infected excisional wounds to evaluate wound healing and bacterial load reduction over 14 days. The synthesized QDs were spherical with an average size of less than 10 nm. Ag-QDs exhibited a lower MIC (average: 125 µg/mL) compared to ZnO-QDs (average: 275 µg/mL) against both bacteria. Both QDs significantly inhibited biofilm formation ($p<0.05$). Gene expression analysis revealed that Ag QDs caused a more pronounced downregulation of biofilm genes (2.5 to 5-fold reduction) compared to ZnO-QDs (1.5 to 3-fold reduction). In the mouse model, wounds treated with Ag-QDs showed superior healing rates, reduced inflammation, and a more significant decrease in bacterial load compared to ZnO-QDs and the antibiotic control group. Biosynthesized Ag-QDs and ZnO-QDs demonstrate significant anti-biofilm and wound-healing properties. Ag-QDs showed greater potency in inhibiting biofilm gene expression and promoting wound healing in *S. aureus* and *A. baumannii* infections. These findings suggest that quantum dots, particularly Ag-QDs, are promising nanotherapeutic agents against biofilm-associated wound infections caused by MDR bacteria.

Please cite this paper as: Nabipour, Y.S., Hesampour, A., Ahmady Asbchin, S., Tajabadi, M., & Rostamzad, A. (2025). Differential modulation of biofilm-associated gene expression by Ag and ZnO quantum dots in gram-positive and gram-negative bacteria: implications for cutaneous wound healing. *Journal of Genetic Resources*, 11(2), 268-276. doi: *10.22080/jgr.2026.31027.1456*

Introduction

The World Health Organization (WHO) has classified antimicrobial resistance (AMR) as one of the greatest threats to global health in the 21st century. This phenomenon, accelerated by the inappropriate and excessive use of antibiotics in medicine and agriculture, undermines our ability

to treat common infections and jeopardizes the achievements of modern medicine (Ferdinand *et al.*, 2024). It is estimated that infections caused by antibiotic-resistant bacteria result in millions of deaths annually worldwide and impose a substantial economic burden on healthcare systems.

Among resistant bacteria, a group of pathogens known as ESKAPE (including *Enterococcus faecium*, *Staphylococcus aureus*, *Klebsiella pneumoniae*, *Acinetobacter baumannii*, *Pseudomonas aeruginosa*, and *Enterobacter* spp.) is of particular importance. These bacteria are recognized as a silent crisis in healthcare settings due to their inherent ability to "escape" the microbicidal effects of common antibiotics and even last-line defenses (Kaiser *et al.*, 2023). One of the most critical mechanisms these pathogens employ to survive in stressful environments and establish chronic infections is their capacity to form biofilms.

Biofilms are complex, dynamic structures formed through several stages: initial attachment of bacteria to a biotic or abiotic surface, proliferation and microcolony formation, production of an extracellular polymeric matrix (EPS) primarily composed of polysaccharides, proteins, and DNA, and finally, maturation and dispersion of cells to colonize new surfaces (Sharma *et al.*, 2023). This sessile mode of life confers a tremendous survival advantage to bacteria, increasing their resistance to antibiotics by up to 1000-fold (Ghaioumy *et al.*, 2021).

The EPS matrix not only acts as a physical barrier against antibiotic penetration but also facilitates cell-to-cell communication via quorum-sensing systems within a stable microenvironment and enhances the exchange of resistance genes among bacteria. Consequently, biofilms serve as reservoirs for the persistence of resistant bacteria, rendering the complete eradication of infections using conventional methods nearly impossible (Sharma *et al.*, 2023). This characteristic poses a major challenge in treating infections associated with medical implants (such as catheters and prostheses) and chronic wounds (particularly diabetic and burn wounds). Pathogens, like *Staphylococcus aureus* and *Acinetobacter baumannii*, are primary agents of these difficult-to-treat infections (Ciofu *et al.*, 2012; Abdelmoneim *et al.*, 2023).

In *Staphylococcus aureus*, the biofilm formation process is primarily mediated by the ica (intercellular adhesin) operon. This operon includes the *icaA* and *icaD* genes responsible for synthesizing polysaccharide intercellular adhesin (PIA) or poly-N-acetylglucosamine (PNAG). PIA plays a key role in cell-to-cell adhesion and the formation of the multilayer biofilm structure (Frank *et al.*, 2007). On the other hand, in *Acinetobacter baumannii*, renowned for its high intrinsic and acquired resistance to a wide range of antibiotics, other virulence factors are involved in biofilm formation. Key among these is the biofilm-associated protein (Bap), a large surface protein involved in biofilm maturation and stability, and the outer membrane protein A (OmpA). Besides its structural role in the membrane, OmpA is also implicated in initial surface attachment, invasion of epithelial cells, and induction of host cell death (Rezania *et al.*, 2022; Barati *et al.*, 2024). Therefore, targeting these key genes' expression represents a strategic approach to combating biofilm-related infections.

In recent years, nanotechnology has emerged as a promising horizon for addressing the antimicrobial resistance crisis. In this context, quantum dots (QDs), which are semiconductor nanoparticles typically 2-10 nm in size with unique optical and electronic properties (Farzin *et al.*, 2020), as well as metal and metal oxide nanoparticles, have garnered significant attention. Silver nanoparticles (AgNPs) and zinc oxide nanoparticles (ZnO NPs) are well-known for their broad-spectrum antimicrobial activity. The primary mechanisms of action of these nanoparticles include the generation of reactive oxygen species (ROS), causing oxidative stress and damage to cellular macromolecules, disruption of the bacterial cell membrane through electrostatic interaction, and interference with vital cellular processes such as DNA replication and protein synthesis (Patra *et al.*, 2014; Thangamuthu *et al.*, 2019).

Various methods are employed for the synthesis of nanoparticles, which can be broadly categorized into physical, chemical, and biological approaches. Physical methods, such as laser ablation and sputtering, often require high energy consumption and specialized equipment. Chemical methods, including chemical reduction, sol-gel, and hydrothermal synthesis, offer better

control over nanoparticle size and morphology but may involve toxic reagents and generate hazardous byproducts. Among these, the hydrothermal method, which involves chemical reactions in aqueous solutions at elevated temperatures and pressures, is considered a modern and versatile technique for producing high-quality nanoparticles with controlled crystallinity and purity (Harish *et al.*, 2022). Biological or green synthesis methods, utilizing plant extracts or microorganisms, have gained significant attention as eco-friendly, cost-effective, and biocompatible alternatives. Plant extracts, including those from oak fruit, are rich in bioactive compounds such as phenols and flavonoids, which can act as both reducing and capping (stabilizing) agents in nanoparticle synthesis, thereby reducing toxicity and enhancing biocompatibility (Pomastowski *et al.*, 2020). This study employed the green synthesis approach to produce silver and zinc oxide quantum dots. Although numerous studies have investigated the individual antibacterial effects of silver or zinc oxide nanoparticles, a clear research gap exists regarding a direct and comprehensive comparison of the efficacy of these two nanoparticles against the expression of genes involved in biofilm formation in key ESKAPE pathogens, and subsequently, evaluating their impact on the healing process of infected wounds in animal models. This study was designed to fill this gap. To fulfill this aim, the green synthesis and detailed physicochemical characterization of Ag-QDs and ZnO-QDs were first performed using oak fruit extract. Subsequently, the anti-biofilm activity of these two nanoparticles were compared at the phenotypic (quantitative and qualitative assessment of biofilm formation) and genotypic levels (analysis of the expression levels of *icaA*, *icaD* genes in *Staphylococcus aureus* and *bap*, *ompA* in *Acinetobacter baumannii*). Finally, using a skin wound infection model in laboratory animals, the therapeutic potential of these nanoparticles in accelerating the healing process and eradicating the infection was evaluated.

Materials and Methods

Synthesis and characterization of QDs

This synthesis was carried out using a hydrothermal method with only water as the solvent. Acorns were collected from the oak forests of the Zagros Mountain range. At first, Ag-QDs and ZnO-QDs, as green synthesizers, were synthesized using a hydrothermal method. Briefly, 5g of powdered oak fruit (Quercus spp.) was refluxed in 50 mL of deionized water for 30 min. The extract was filtered and centrifuged. For Ag-QDs, 20 mL of 1 mM $AgNO_3$ solution was added dropwise to 20 mL of the colloidal extract (0.01 mg/mL) under stirring. For ZnO-QDs, 20 mL of the extract was added to 200 mL of 1.5 mM $Zn(NO_3)_2$ solution, followed by pH adjustment to 10-11 using 1M NaOH. The mixtures were incubated in the dark at 60°C for 24 hours. The resulting colloids were centrifuged, washed, and dried at 60°C (Fig. 1).

Then, they were synthesized, characterized, and confirmed by UV/vis spectroscopy (Shimadzu UV-1800). Size, morphology, and distribution were analyzed using Transmission Electron Microscopy (TEM, Zeiss EM900).

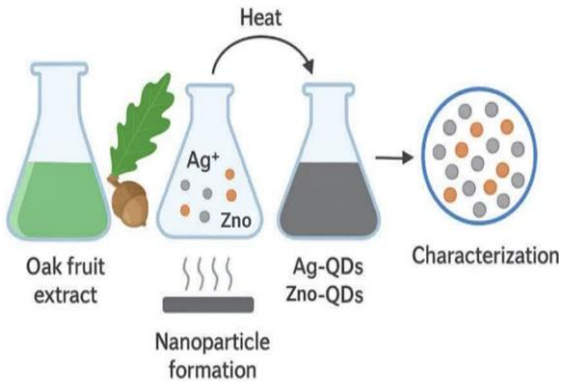

Fig.1. Schematic diagram of the green synthesis process for Ag-QDs and ZnO-QDs quantum dots using oak fruit extract: This schematic illustrates the green synthesis process. The oak fruit extract acts simultaneously as both a reducing and a stabilizing agent. The formation of nanoparticles is initially indicated by a color change and subsequently confirmed through various characterization techniques.

Bacterial strains and culture conditions

In addition to standard strains, a total of 63 clinical samples isolated from wound infections (diabetic, burn, and surgical wounds) were utilized over a period of six months at the laboratory of Razi Hospital in Ilam.

Clinical isolates of *Acinetobacter baumannii* (n= 25) and *Staphylococcus aureus* (n=38) were

collected from wound infections (diabetic, burn, surgical). Standard strains *A. baumannii* PTCC 1797 and *S. aureus* ATCC 29213 were used as controls. Bacteria were identified by conventional biochemical tests and cultured in Tryptic Soy Broth (TSB) or on Tryptic Soy Agar (TSA) at 37°C.

Antibacterial susceptibility testing

The (MIC) of Ag-QDs and ZnO-QDs was determined using the broth microdilution method according to CLSI guidelines (Parvekar *et al.*, 2020). The minimum bactericidal concentration (MBC) was determined by subculturing from wells showing no visible growth.

Biofilm formation assay

Biofilm formation was quantified using the microtiter plate (MTP) assay (Ghanayem *et al.*, 2025). Bacterial suspensions (0.5 McFarland) were added to 96-well plates and incubated for 24 h. After washing, adherent biofilms were stained with 1% crystal violet, eluted with acetic acid, and the optical density (OD) was measured at 570 nm. Isolates were classified as strong, moderate, weak, or non-biofilm producers.

Anti-biofilm activity of QDs

The ability of sub-MIC concentrations of QDs to inhibit biofilm formation was evaluated using the MTP assay. Bacteria were grown in the presence of QDs, and biofilm biomass was quantified as described above.

Gene expression analysis by Real-time PCR

Biofilm-positive strains were treated with sub-MIC concentrations of Ag-QDs or ZnO-QDs for 6 hours. Total RNA was extracted using the RNeasy Mini Kit (Qiagen). cDNA was synthesized using the PrimeScript RT Reagent Kit (Takara).

Real-time PCR: Gene expression of *bap* and *ompA* (*A. baumannii*), and *icaA* and *icaD* (*S. aureus*) was analyzed using SYBR Green master mix (Bioneer) on a Rotor-gene Q instrument (Qiagen). The 16S rRNA gene was used as an internal control. Primer sequences are listed in Table 1. Relative gene expression was calculated using the 2^(-ΔΔCt) method (Siasi *et al.*, 2020).

Table 1. Primer sequences used for Real-time PCR.

Genes	Primers	Oligomer (5'→3')	Length (bp)	References
ica A	F	TCTCTTGCAGGAGCAATCAA	188	Mehta *et al.*, 2022
	R	TCAGGCACTAACATCCAGCA		
ica D	F	ATGGTCAAGCCCAGACAGAG	225	Mahjobipoor *et al.*, 2022
	R	CGTGTTTTCAACATTTAATGCAA		
bap	F	TGAAAGTGGCTGCCAGTGAT	223	Asaei *et al.*, 2020
	R	TCTGCGTCAGCGTCACTATC		
ompA	F	GCTGGTGTTGGTGCTTTCTG	490	Asaei *et al*., 2020
	R	TCGGTTGATCCCAAGCGAAA		
16S rRNA Universal	F	AACCTACCTATAAGACTGGG	570	Ghanayem *et al.*, 2025
	R	CATTTCACCGCTACACATGG		

***In vivo* wound healing study**

Sixty female *Balb/c* mice (18-22g) were anesthetized, and a full-thickness excisional wound (10x10 mm²) was created on the dorsum. Wounds were inoculated with 100 µL of bacterial suspension (10^6 CFU/mL) of either *A. baumannii* or *S. aureus*. After 48 hours, mice were randomly divided into groups (n=3 per group per pathogen): Group 1: Untreated control (infected), Group 2: Treated with Ag-QDs (200 µg/mL), Group 3: Treated with ZnO-QDs (300 µg/mL), and Group 4: Treated with standard antibiotic (Ciprofloxacin for *A. baumannii*, Cefixime for *S. aureus*). Treatments (50 µL) were applied topically once daily for 14 days. Wound area was measured on days 0, 2, 5, 8, 11, and 14. The percentage of wound contraction was calculated. Bacterial load in the wound was assessed by swabbing and colony counting on day 14. Blood samples were analyzed for hematological changes.

The study was approved by the Ilam University of Medical Sciences Ethics Committee (IR.ILAM.REC.1401.008). To evaluate the healing process, wound dimensions were measured from the first day of infection induction and on days 0, 2, 5, 8, 11, and 14 post-infection. To quantify the percentage of wound closure, X-axis and Y-axis measurements were performed

for each mouse individually. These values were then used to calculate the rhombus area using the equation A = ½ × X × Y. Statistical analyses to assess differences in wound closure were performed using Graphpad Prism 5.

The percentage of wound contraction was determined by measuring the wound area immediately after wound creation and over the 2-week study period on days 0, 2, 5, 8, 11, and 14. The measurement was expressed as the percentage of wound contraction using the following formula:

Statistical analysis

Data were analyzed using SPSS ver.20.0 software and GraphPad Prism ver.20 One-way ANOVA followed by Tukey's post-hoc test was used for comparisons. A p-value of < 0.05 was considered statistically significant. Wound Contraction Percentage= [(Initial wound area on day 0-Wound area on day n) / (Initial wound area on day 0)] × 100

Results

Characterization of QDs

UV/vis spectroscopy showed characteristic absorption peaks for Ag-QDs at~420 nm and for ZnO-QDs at ~370 nm (Fig. 2). TEM analysis confirmed the synthesis of spherical, well-dispersed nanoparticles with an average diameter of 7-9 nm for both types of QDs (Fig. 3).

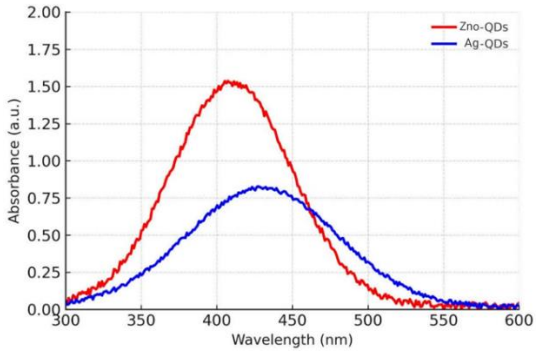

Fig. 2. UV/vis absorption spectra of Ag-QDs and ZnO-QDs: This figure presents the ultraviolet-visible (UV/vis) absorption spectra of the synthesized quantum dots. The presence of distinct characteristic peaks around 400 nm for both samples confirm the successful synthesis of the quantum dots.

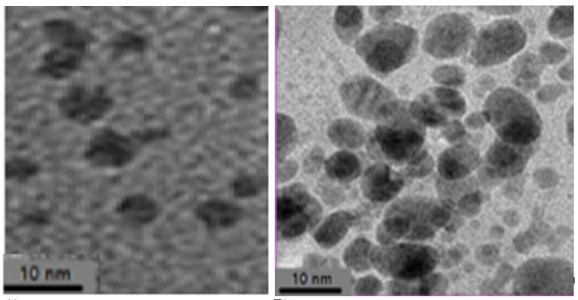

Fig. 3. Illustrating a TEM micrograph of the spherical morphology and nanoscale distribution of synthesized quantum dots: A) ZnO-QDs; B) Ag-QDs.

Antibacterial activity

Ag-QDs exhibited stronger antibacterial activity than ZnO-QDs.The average MIC values for Ag-QDs were 200 µg/mL against *S. aureus* and 300 µg/mL against *A. baumannii*. The average MIC values for ZnO-QDs were 300 µg/mL and 400 µg/mL against *S. aureus* and *A. baumannii*, respectively. The MBC values were generally 2-4 times higher than the MICs.

Biofilm inhibition

Both QDs significantly reduced biofilm formation at sub-MIC levels. Ag QDs caused a 65-75% reduction in biofilm biomass, while ZnO-QDs caused a 45-60% reduction compared to untreated controls ($p<0.05$). *S. aureus* biofilms were slightly more susceptible to inhibition than *A. baumannii* biofilms (Fig. 4).

Effect on biofilm gene expression

Real-time PCR analysis revealed that treatment with sub-MIC concentrations of QDs significantly downregulated the expression of biofilm-related genes (Fig. 5).

In *S. aureus*, Ag-QDs reduced *icaA* and *icaD* expression by 4.8-fold and 5.2-fold, respectively. ZnO-QDs reduced their expression by 2.7-fold and 3.1-fold. In *A. baumannii*, Ag-QDs reduced *bap* and *ompA* expression by 3.5-fold and 4.1-fold. ZnO-QDs reduced their expression by 1.8-fold and 2.5-fold. The downregulation caused by Ag-QDs was significantly greater than that caused by ZnO-QDs for all target genes($p<0.05$).

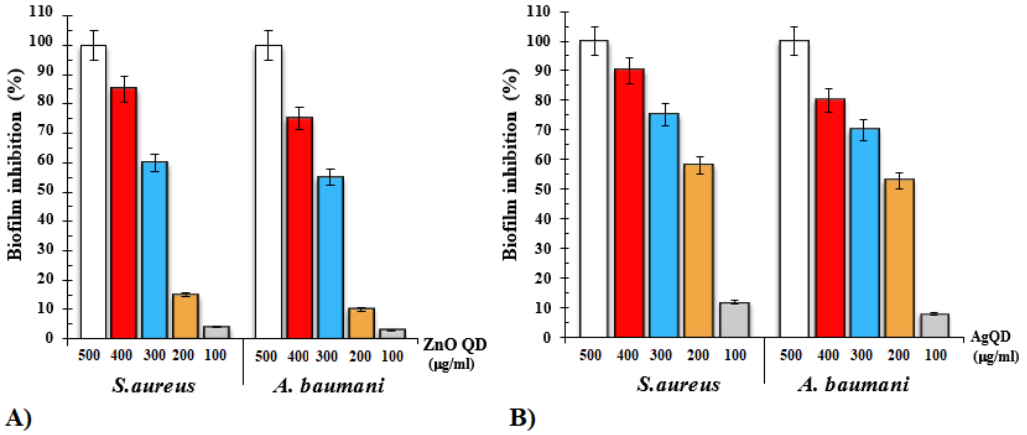

Fig. 4. The effect of quantum dots on inhibiting growth and biofilm in strong biofilm-producing clinical isolates of *S. aureus* and *A. baumanni*: A) Silver quantum dots; B) Zinc oxide quantum dots (Statistical differences were analyzed using one-way ANOVA followed by Tukey's post hoc test, with $p < 0.05$ considered statistically significant).

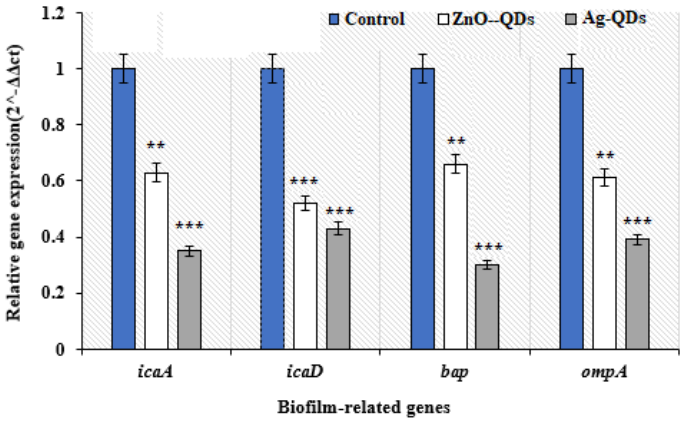

Fig 5. Effect of Sub-MIC silver and zinc oxide quantum dots on the expression of biofilm-associated genes in *S. aureus* and *A.baumannii*: Both Ag-QDs and ZnO-QDs significantly downregulated the expression of the target genes compared to the untreated control ($p < 0.05$), with Ag-QDs demonstrating a more potent inhibitory effect.

Wound healing in mice

Wounds treated with Ag-QDs showed the fastest rate of contraction from day 5 onwards, achieving near-complete closure by day 14. The ZnO-QD and antibiotic groups showed intermediate healing, while the untreated control groups healed the slowest (Figure 5). Topical application of Ag-QDs resulted in the most substantial reduction in wound bacterial load (≈4 log reduction), followed by ZnO-QDs (≈3 log reduction) and antibiotics (≈2.5 log reduction) (Fig. 6).

Macroscopic studies showed that Ag-QD-treated wounds displayed less erythema, edema, and exudate compared to other groups. No significant adverse changes in white blood cell counts or red blood cell morphology were observed in any treatment group compared to controls.

Discussion

The escalating crisis of AMR, compounded by the protective nature of biofilms, necessitates the exploration of novel antimicrobials like QDs (Zou *et al.*, 2016). Our study successfully synthesized Ag and ZnO- QDs via a green, sustainable method using oak fruit extract. The small size (<10 nm) of the QDs is advantageous for penetrating bacterial cells and biofilm matrices (Shahbazi *et al.*, 2023).

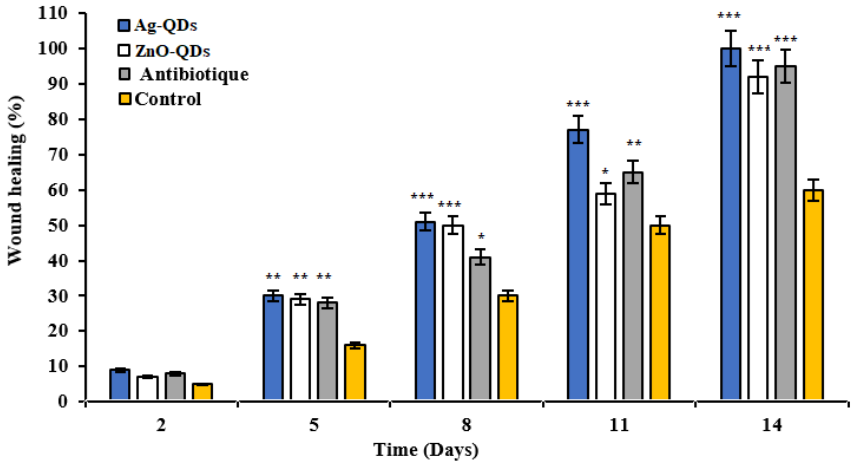

Fig. 6 Wound healing progression in *S. aureus* and *A. baumannii* infected mice following treatment with Ag-QDs, ZnO-QDs compared to antibiotic therapy: the figure illustrates the temporal progression of wound healing in infected murine models treated with Ag-QDs, ZnO-QDs, and standard antibiotic therapy. Wound assessment was performed on post-treatment days 2, 5, 8, 11, and 14. Both quantum dot formulations demonstrated a statistically significant enhancement in wound closure and tissue repair compared to the untreated control group.

The superior antibacterial and anti-biofilm potency of Ag-QDs over ZnO-QDs, as evidenced by lower MICs and greater biofilm inhibition, aligns with previous reports on the strong biocidal activity of silver ions and nanoparticles (Nandhini *et al.*, 2024). The enhanced activity may be attributed to Ag^+ ions' ability to disrupt multiple cellular functions, including membrane integrity, enzyme activity, and DNA replication (Pino *et al.*, 2023).

The key novel finding of this study is the differential impact of QDs on the genetic regulation of biofilm formation. The significant downregulation of *icaA/D* in *S. aureus* and *bap/ompA* in *A. baumannii* by Ag-QDs suggests they interfere with quorum sensing or key regulatory pathways governing biofilm matrix production (Afrasiabi *et al.*, 2024). ZnO-QDs also reduced gene expression but to a lesser extent, possibly linked to their primary mechanism of ROS generation rather than direct genetic interference (Kaiser *et al.*, 2023). This genotypic inhibition correlates with the observed phenotypic reduction in biofilm mass.

The *in vivo* wound healing results strongly support the therapeutic potential of QDs, particularly Ag-QDs. The accelerated healing can be attributed to a combination of factors: 1) Effective reduction of the bacterial bioburden, preventing ongoing infection and inflammation; 2) Possible anti-inflammatory effects of the QDs; and 3) Potential stimulation of fibroblast proliferation and angiogenesis by released metal ions, as suggested in other studies (Hakimzadeh *et al.*, 2024). The superior performance of Ag-QDs over standard antibiotics highlights their potential as alternatives in treating MDR wound infections (Melkumyan *et al.*, 2024).

The absence of significant hematological toxicity is encouraging for future translational applications, although long-term toxicity studies are required.

Conclusion

This comparative study demonstrates that biosynthesized Ag-QDs and ZnO-QDs are effective against MDR, biofilm-forming pathogens. Ag-QDs exhibited superior antibacterial, anti-biofilm (both phenotypic and genotypic), and wound-healing properties compared to ZnO-QDs. The ability of Ag-QDs to downregulate critical biofilm genes in *S. aureus* and *A. baumannii* provides a mechanistic insight into their mode of action. These findings position Ag-QDs, synthesized via an eco-friendly route, as

a promising nanotherapeutic candidate for managing challenging biofilm-associated wound infections. Future research should focus on mechanistic details of gene regulation, formulation into stable wound dressings, and comprehensive in vivo safety profiling.

Conflict of interest

The authors declare that there are no conflicts of interest.

References

Abdelmoneim, A., Ali, R., Abdelhafeez, A., Khallaf, A., Molham, F. M., &Tohamy Abdel-Aziz, M. A. (2023). Detection of ica C gene involved in biofilm formation in methicillin-resistant *Staphylococcus aureus* (MRSA) isolates. *Egyptian Journal of Medical Research*, 4(4), 63-77. https://doi.org/10.21608/ejmr.2023.218352.1408

Afrasiabi, S., & Partoazar, A. (2024). Targeting bacterial biofilm-related genes with nanoparticle-based strategies. *Frontiers in Microbiology*, 15, 1387114. https://doi.org/10.3389/fmicb.2024.1387114

Asaei, Y., & Nowroozi, J. (2020). Isolation of TEM beta-lactamase gene in Pseudomonas aeruginosa and imipenem effect on expression of TEM Gene by Real-time PCR from burn wound samples. *Journal of Military Science and Tactics of Hormozgan University of Medical Sciences*, 8(2), 1-13. http://jms.thums.ac.ir/article-1-802-fa.html

Barati, H., Fekrirad, Z., Jalali Nadoushan, M., &Rasooli, I. (2024). Anti-ompA antibodies as potential inhibitors of *Acinetobacter baumannii* biofilm formation, adherence to, and proliferation in A549 human alveolar epithelial cells. *Microbial Pathogenesis*, 186, 106473. https://doi.org/10.1016/j.micpath.2023.106473

Ciofu, O., Mandsberg, L. F., Wang, H., & Høiby, N. (2012). Phenotypes selected during chronic lung infection in cystic fibrosis patients: Implications for the treatment of Pseudomonas aeruginosa biofilm infections. *FEMS Immunology & Medical Microbiology*, 65(2), 215-225. https://doi.org/10.1111/j.1574-695X.2012.00983.x

Farzin, M. A., &Abdoos, H. (2020). A critical review on quantum dots: From synthesis toward applications in electrochemical biosensors for determination of disease-related biomolecules. *Talanta*, 224, 121828. https://doi.org/10.1016/j.talanta.2020.121828

Ferdinand, A. S., McEwan, C., Lin, C., Betham, K., Kandan, K., Tamolsaian, G., … & Gilkerson, J. (2024). Development of a cross-sectoral antimicrobial resistance capability assessment framework. *BMJ Global Health*, 9, 013280. https://doi.org/10.1136/bmjgh-2023-013280

Frank, K. L., &Patel, R. (2007). Poly-N-acetylglucosamine is not a major component of the extracellular matrix in biofilms formed by icaADBC-positive *Staphylococcus lugdunensis* isolates. *Infection and Immunity*, 75(10), 4728-4742. https://doi.org/10.1128/IAI.00640-07

Ghaioumy, R., Tabatabaeifar, F., Mozafarinia, K., Arabi Mianroodi, A., Isaei, E., Morones-Ramírez, J. R., ... & Kalantar-Neyestanaki, D. (2021). Biofilm formation and molecular analysis of intercellular adhesion gene cluster (icaABCD) among *Staphylococcus aureus* strains isolated from children with adenoiditis. *Iranian Journal of Microbiology*, 13(4), 458-463. https://doi.org/10.18502/ijm.v13i4.6969

Ghanayem, H. R., Tolba, K., &El-Shemy, M. M. G. (2025). Synergistic effect of electrolyzed oxidized water (EO) and peroxyacetic acid on plasmid-mediated quinolone resistance genes of *Pseudomonas aeruginosa*. *World Journal of Microbiology and Biotechnology*, 41, 199. https://doi.org/10.1007/s11274-025-04384-w

Hakimzadeh, S., & Kosar, M. (2024). Wound healing activity of green synthesized copper nanoparticles through cell proliferation-migration, antimicrobial effects, and nitric oxide triggering. *Archives of Razi Institute*, 79(3), 639-644. https://doi.org/10.32592/ARI.2024.79.3.639

Harish, V., Ansari, M. M., Tewari, D., Gaur, M., Yadav, A. B., García-Betancourt, M. L., ... & Barhoum, A. (2022). Nanoparticle and nanostructure synthesis and controlled growth methods. Nanomaterials, 12(18), 3226. https://doi.org/10.3390/nano12183226

Kaiser, K. G., Delattre, V., Frost, V. J., Buck, G. W., Phu, J. V., Fernandez, T. G., & Pavel, I. E. (2023). Nanosilver: an old antibacterial agent with great promise in the fight against

antibiotic resistance. *Antibiotics*, 12(8), 1264. https://doi.org/10.3390/antibiotics12081264

Mahjobipoor, H., Sajadi, M., Honarmand, A., Rahimi-Varposhti, M., Yadegari, L., Attarzadeh, A., ... & Fattahpour, S. (2022). A comparison of disk diffusion method and E-test in determining the susceptibility and resistance of Klebsiella and Acinetobacter strains to cefepime in patients with ventilator-associated pneumonia admitted to the intensive care unit. *Immunopathologia Persa*, 10(2), e30330-e30330. https://doi.org/10.34172/ipp.2022.30330

Mehta, A., Jain, A., & Saxena, G. (2022). *In vitro* antibacterial activity of ethanolic extract of neem leave (Azadirachta indica Linn) against clinical isolates. *Pharmaceutical and Biomedical Research*, 8(4), 301-310. https://doi.org/10.32598/PBR.8.4.1067.1

Melkumyan, V. A., Kurbanova, D. A., Magomedgadzhieva, R. S., Khidiryan, M. V., Eremin, S. A., & Stepanenko, V. S. (2024). Assessment of wound-healing activity of zinc oxide nanoparticles. *Journal of Advanced Pharmacy Education and Research*, 14(1), 73-76. https://doi.org/10.51847/0SQk1Cmx1X

Nandhini, J., Karthikeyan, E., & Elizabeth Rani, E. (2024). Advancing engineered approaches for sustainable wound regeneration and repair: Harnessing the potential of green synthesized silver nanoparticles. *Engineered Regeneration*, 5(3), 306-325. https://doi.org/10.1016/j.engreg.2024.06.004

Parvekar, P., Palaskar, J., Metgud, S., Maria, R., & Dutta, S. (2020). The minimum inhibitory concentration (MIC) and minimum bactericidal concentration (MBC) of silver nanoparticles against *Staphylococcus aureus*. *Biomaterial Investigations in Dentistry*, 7(1), 105-109. https://doi.org/10.1080/26415275.2020.1796674

Patra, P., Roy, S., Sarkar, S., Mitra, S., Pradhan, S., Debnath, N., & Goswami, A. (2014). Damage of lipopolysaccharides in outer cell membrane and production of ROS-mediated stress within bacteria makes nano zinc oxide a bactericidal agent. *Applied Nanoscience*, 5, 857-866. https://doi.org/10.1007/s13204-014-0389-z

Pino, P., Bosco, F., Mollea, C., & Onida, B. (2023). Antimicrobial nano-zinc oxide biocomposites for wound healing applications: A review. *Pharmaceutics*, 15(3), 970. https://doi.org/10.3390/pharmaceutics15030970

Pomastowski, P., Król-Górniak, A., Railean-Plugaru, V., & Buszewski, B. (2020). Zinc oxide nanocomposites-extracellular synthesis, physicochemical characterization and antibacterial potential. *Materials*, 13(19), 4347. https://doi.org/10.3390/ma13194347

Rezania, N., Rahmati, P., Noorbakhsh, F., Farhadyar, N., & Lotfali, E. (2022). Investigation the effects of silver nanoparticles and gold nanoparticles on expression of bap and csu genes in biofilm formation of *Acinetobacter baumannii*. *Iranian Journal of Microbiology*, 14(4), 510-517. https://doi.org/10.18502/ijm.v14i4.10237

Shahbazi, A., & Dall, E. (2023). Synthesis of quantum carbon dots (CQDs) from hard walnut skin by hydrothermal method. *Amirkabir Journal of Civil Engineering*, 55(3), 493-504. https://doi.org/10.22060/ceej.2023.21041.7614

Sharma, S., Mohler, J., Mahajan, S. D., Schwartz, S. A., Bruggemann, L., & Aalinkeel, R. (2023). Microbial biofilm: a review on formation, infection, antibiotic resistance, control measures, and innovative treatment. Microorganisms, 11(6), 1614. https://doi.org/10.3390/microorganisms11061614

Thangamuthu, M., Hsieh, K. Y., Kumar, P. V., & Chen, G. Y. (2019). Graphene- and graphene oxide-based nanocomposite platforms for electrochemical biosensing applications. *International Journal of Molecular Sciences*, 20(12), 2975. https://doi.org/10.3390/ijms20122975

Zou, X., Zhang, L., Wang, Z., & Luo, Y. (2016). Mechanisms of the antimicrobial activities of graphene materials. *Journal of the American Chemical Society*, 138(7), 2064-2077. https://doi.org/10.1021/jacs.5b11411